Preparation and Characterisation of Optimised Hydrochar from Hydrothermal Carbonisation of Macadamia Shells

Fangyu Fan,[a,b,*] Zhifeng Zheng,[c] Yun Liu,[a,b] Yuanbo Huang,[c] and Zhengjun Shi [d,*]

The yield of macadamia shells (MSs) is huge. The preparation of hydrochar of MSs for the purpose of energy has broad prospects. This study investigated the possible optimum conditions for the most appropriate yield and higher heating value (HHV) of hydrochar through hydrothermal carbonisation (HTC) of MSs. The yield and HHV *via* HTC were systematically analysed by response surface methodology (RSM) using a synthetic weighted scoring method. The operating parameters included reaction temperature, reaction time, and water-to-biomass ratio. According to the mathematical model of RSM, the maximum response value was obtained under the following optimum conditions: reaction temperature, 220 °C; reaction time, 60 min; and water-to-biomass ratio, 11. The results showed that the reaction temperature exerted more remarkable influence than time and water-to-biomass ratio. Under the optimal conditions, the hydrochar yield and HHV were 57.58% and 22.69 MJ/kg, respectively. The results of elemental, proximate, Brunauer–Emmett–Teller, scanning electron microscopy, and Fourier transform infrared spectroscopy analyses showed that the hydrochar fuel properties improved compared with those of raw MSs. Furthermore, the surface structure and functional groups changed.

Keywords: Macadamia shells; Hydrothermal carbonisation; Hydrochar; Response surface methodology; Characterisation

Contact information: a: School of Light Industry and Food Engineering, Southwest Forestry University, 650224 Kunming, People's Republic of China; b: Key Laboratory for Forest Resources Conservation and Utilisation in the Southwest Mountains of China, Ministry of Education, Southwest Forestry University, 650224 Kunming, Yunnan, People's Republic of China; c: College of Materials Engineering, Southwest Forestry University, 650224 Kunming, People's Republic of China; d: School of Chemical Engineering, Southwest Forestry University, 650224 Kunming, People's Republic of China;
** Corresponding authors: ffy118@163.com (Fangyu Fan); shizhengjun1979@163.com (Zhengjun Shi)*

INTRODUCTION

Sustainable energy sources, such as biomass, have attracted attention worldwide with the increasing demand for fossil fuels and growing concerns about environmental pollution from fossil fuels (Yang *et al*. 2015). To date, the sustainable management of waste from the agricultural and forestry processing sectors has been a global challenge (Nizamuddin *et al*. 2015). Hence, generating energy from agricultural and forestry wastes is of great significance. In China, various kinds of agricultural and forestry wastes are produced annually, and the output is large (Zhao *et al.* 2016). Macadamia shells (MSs) are an example of agricultural and forestry wastes with large output (Fan *et al.* 2017a; Kumar *et al.* 2017). China has initiated the development of the macadamia industry and the production of large amount of MSs. The yield of MSs is approximately 70% of the

harvested mass. Therefore, the utilisation of MSs is a problem that should be solved.

In rural areas of China, MSs are commonly burned as fuel or abandoned as rubbish, which results in severe environmental pollution. The comprehensive utilisation of MSs becomes an important issue. MSs contain considerable amounts of hemicelluloses, cellulose, and lignin (Wechsler *et al.* 2013), and they can be converted to biochar or bio-oil as fuels by thermochemical processes (Abdulrazzag *et al.* 2014; Fan *et al.* 2017b). Many studies pertaining to carbon-material-derived MSs *via* different methods have been reported. Wongcharee *et al.* (2017) prepared a magnetite nanosorbent from magnetite nanoparticles and biochar of MSs using CO_2 activation at 900 °C. The magnetite nanosorbent showed excellent adsorption capacities. Zheng *et al.* (2017) prepared a high-performance sodium battery using MSs, with an ICE of 91.4% and real specific capacity of 314 mAh/g. Rajarao and Sahajwalla (2016) synthesised silicon carbide and silicon nitride nanopowders using MSs as the source of carbon. Nevertheless, biochar preparation using MSs is rarely reported due to its low output. Fan *et al.* (2017a) investigated the combustion kinetics of biochar prepared by pyrolysis of MSs, showing that biochar can be prepared as a fuel from MSs.

Hydrothermal carbonisation (HTC) is a biomass thermochemical conversion process that has several advantages. HTC is performed in the temperature range of 180 °C to 260 °C and the time range of 5 to 240 min, during which the biomass is submerged in water (Kambo and Dutta 2015; Nizamuddin *et al.* 2016a; Fan *et al.* 2017b). Along with the wide availability of raw materials, HTC exhibits remarkable benefits, such as simplicity, relatively mild reaction conditions, and less greenhouse gas emissions compared with pyrolysis (Xing *et al.* 2016). Recent studies on HTC have used a wide range of biomass feedstock, such as *Miscanthus* (Kambo and Dutta 2015), corn straw (Xing *et al.* 2016), oil palm shell (Nizamuddin *et al.* 2016a), and *Camellia oleifera* shells (Fan *et al.* 2017b). The HTC mechanism is associated with a series of hydrolysis, condensation, decarboxylation, and dehydration reactions (Nizamuddin *et al.* 2017). The calorific value of hydrochar can be compared to highly ranked coals (Thangalazhy-Gopakumar *et al.* 2015). The HTC process is dependent on reaction temperature, reaction time, water-to-biomass ratio value (ratio value of mass), and feedstock (Nizamuddin *et al.* 2017). The effects of these conditions on the hydrothermal carbonization of MSs are analyzed in this paper.

Most studies have focused on the analysis of the characteristics of hydrochar; however, research on the process of HTC is lacking. The aim of this preliminary work was to optimise the parameters of hydrochar production using HTC from MSs. In addition, hydrochar and MSs were analysed using higher heating value (HHV), elemental analysis, proximate analysis, Brunauer–Emmett–Teller (BET), scanning electron microscopy (SEM), and Fourier transform infrared spectroscopy (FTIR). Preparation of hydrochar from MSs, which provides a new idea for the comprehensive utilization of MSs.

EXPERIMENTAL

Materials

MSs were collected from Yunnan province, China. MSs were washed with tap water and then distilled water to remove impurities. The washed MSs were oven-dried at 105 °C for 24 h. Dried MSs were ground into pieces of less than 0.6 mm.

Hydrochar Preparation

HTC hydrochar was prepared in a laboratory scale semibatch 500 mL Parr autoclave reactor. The parameters ranged within a temperature of 180 °C to 260 °C, reaction time of 30 to 180 min, and water-to-biomass ratio of 6 to 14. The selection of parameters for HTC was based on previous studies (Kambo and Dutta 2015; Nizamuddin *et al.* 2016a; Xing *et al.* 2016; Nizamuddin *et al.* 2017). The HHV of the hydrochar under the studied conditions is close to or better than that of lignite (Liu *et al.* 2016).

Approximately 50 g of the powder MSs was combined with deionised water in the batch reactor. The reactor was flooded with nitrogen under high pressure to remove oxygen. This process was repeated five times. Subsequently, the reactor was heated to the desired temperature and maintained for various periods of time. To terminate the reaction, the reactor was immersed in water to cool it to room temperature. Finally, the reaction mixture was filtered through a G-4 glass filter to obtain the solid product (hydrochar). The hydrochar was dried at 105 °C for 24 h and preserved hermetically (Xing *et al.* 2016).

Experimental Design Using Response Surface Methodology (RSM)

To optimise the HTC conditions for MSs, a 3^K factorial Box–Behnken design (BBD) was applied. The BBD is an efficient method to estimate quadratic polynomials and combine values for optimisation of the response within a 3D observation space (Ferdosian *et al.* 2014; Jung *et al.* 2016). The reaction temperature, time, and water-to-biomass ratio were used as the independent variables of the BBD to study the effects of reaction conditions on HTC from MSs (Table 1). Seventeen experiments were suggested for the experimental design for the production of hydrochar from MSs. The response of each run was further studied by using the Design-Expert software 8.0 (STAT-EASE., Minneapolis, MN, USA) to optimise the reaction conditions.

Table 1. Levels for the Box–Behnken Design

Factor	Temperature (*A*)	Time (*B*)	Water-to-Biomass Ratio (*C*)
Unit	°C	min	
High	260	180	12
Low	180	60	8
High coded	1	1	1
Low coded	−1	−1	−1

Given that the yield and HHV of the hydrochar showed an inverse relation, a synthetic weighted scoring method was used as the response value for reasonable hydrochar produced. The maximum yield or HHV was 100, and the minimum was 0 for the 17 experiments. The yield or HHV was used as abscissa, and the score was the vertical coordinate. The highest and lowest scores were also included, and the linear equation of yield or HHV was obtained. The yield or HHV of the response surface test was taken into account, and the corresponding comprehensive evaluation of the score was determined. Yield and HHV are equally important to evaluate the quality of hydrochar, and their weighted coefficient is 0.5. The synthetic score was obtained using Eq. 1.

$$\text{Synthetic score} = \text{yield score} \times 0.5 + \text{HHV} \times 0.5 \quad (1)$$

Mass Yield of Hydrochar

The mass yield of the hydrochar was calculated using Eq. 2 as follows,

$$\text{Hydrochar yield } \% = (W_{\text{hydrochar}} / W_{\text{MSs}}) \times 100 \quad (2)$$

where $W_{\text{hydrochar}}$ is the mass of dry hydrochar, and W_{MSs} is the mass of dry MSs.

Research Methodology

The elemental analysis (C, H, N, and S) was performed using a Vario EL III elemental analyser (Elementar, Langenselbold, Germany). The oxygen content was calculated using the difference. Proximate analysis was performed using a 5E-MAG6600 automatic proximate analyser (Instruments Co., Ltd., Changsha, China). The HHV was tested using a bomb calorimeter (IKA C2000 basic, Staufen, Germany). BET characteristics of the samples were analysed using a BET analyser (Micrometrics ASAP 2020, Norcross, GA, USA). For SEM measurements, the samples were sputter coated with Pt and examined with a JSM-6490LV scanning electron microscope (JEOL, Tokyo, Japan). The functional groups were determined by FTIR spectra analysis (Magna-IR 560 ESP Thermo Nicolet, Waltham, MA, USA). The sample discs were prepared by mixing the dried samples with KBr powder at room temperature at a sample/KBr ratio of 1:200.

RESULTS AND DISCUSSION

Effect of Process Parameters on Hydrochar Production

The treatment conditions of the hydrochar were investigated to maximize its yield and HHV. Figure 1(a) shows the effect of the temperature during HTC at 120 min and water-to-biomass ratio of 10. With increasing temperature, the yield decreased, and the HHV increased, demonstrating that temperature plays an important role. Volatile matter is released at high temperatures, which intensifies the elimination and dehydration, resulting in reduced hydrochar mass (Kim *et al.* 2016; Mau *et al.* 2016). The carbon content increased, and the oxygen content decreased, which increased the HHV. Similar phenomena were observed in previous studies (Liu *et al.* 2012; Lei *et al.* 2015).

HTC is a slow reaction process occuring over minutes to days (Nizamuddin *et al.* 2016b; Nizamuddin *et al.* 2017). In terms of the reaction mechanism, hydrolysis of the extractives, hemicellulose, and cellulose occurs first. Dehydration, decarboxylation, condensation, polymerisation, and aromatisation subsequently occur sequentially in the liquid phase (Reza *et al.* 2015). Hence, the reaction time affects the properties of the HTC products. According to previous reports, the selected test range of reaction time was 30 to 180 min (Nizamuddin *et al.* 2016b; Peng *et al.* 2016). The effect of reaction time on the yield and HHV is shown in Fig. 1(b) at a temperature of 220 °C and water-to-biomass ratio of 10. A higher hydrochar yield was produced at a lower reaction time during HTC. The change in HHV was reversed. This observation is explained by the fact that light components and permanent gases were formed; consequently, the hydrochar showed decreased yield and porous structure (Jain *et al.* 2015, 2016).

The water-to-biomass ratio exerted little influence on the yield and HHV, as shown in Fig. 1(c) at 220 °C and 120 min. A high hydrochar yield was obtained at a low water-to-biomass ratio. In addition, the yield slightly decreased with increasing water-to-biomass ratio. The particle size and biomass concentrations affect the hydrochar yield and HHV (Kambo and Dutta 2014; Álvarez-Murillo *et al.* 2015). The present research ignored the effect of particles during HTC and examined only the effects of concentration.

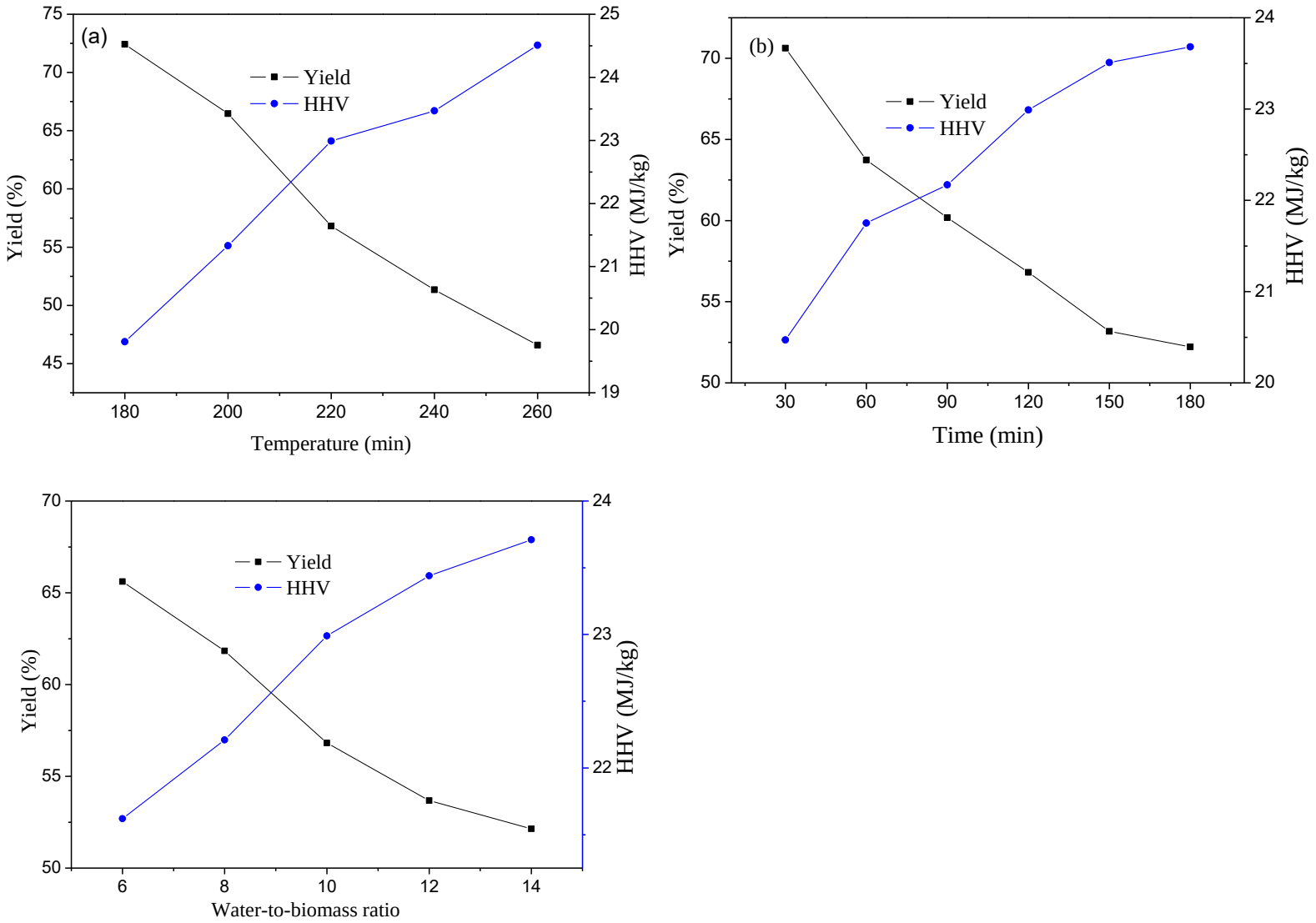

Fig. 1. Effect of (a) reaction temperature, (b) reaction time, and (c) water-to-biomass ratio on the yield and HHV of hydrochar

Statistical Analysis of Hydrochar Production

The reaction temperature, time, and water-to-biomass ratio as operation variables were used in the design analysis to determine optimum conditions. The design matrix for the experiments and the response values are shown in Table 2.

Table 2. Experimental Design Matrix and the Corresponding Hydrochar Yield, HHV, and Response Value

Std.	Run	*A*	*B*	*C*	Hydrochar Yield (%)	HHV (MJ/kg)	Response Value (score)
1	11	−1	−1	0	70.12	20.65	54.17
2	5	1	−1	0	48.83	24.22	56.33
3	10	−1	1	0	63.21	21.98	56.59
4	9	1	1	0	42.02	24.41	47.50
5	12	−1	0	−1	72.29	19.89	50.0
6	2	1	0	−1	58.9	22.4	54.0
7	6	−1	0	1	66.15	21.45	55.92
8	4	1	0	1	40.56	24.89	50.00
9	1	0	−1	−1	57.45	22.65	53.77
10	14	0	1	−1	58.81	22.54	55.26
11	8	0	−1	1	54.86	23.39	57.53
12	16	0	1	1	49.96	23.85	54.41
13[a]	3	0	0	0	56.81	22.99	57.01
14[a]	15	0	0	0	56.11	23.21	56.70
15[a]	13	0	0	0	56.32	23.11	58.03
16[a]	7	0	0	0	56.64	23.04	56.84
17[a]	17	0	0	0	56.81	22.99	56.60

Note: The centre point was replicated five times.

The actual values of the independent factors and response were used to create a model equation. Experimental results were fitted to a linear model and a second-order mathematical model for the synthetic score of hydrochar from MSs. The resulting equation is as follows,

$$\text{Score} = +57.04 - 1.11A - 1.00B + 0.60C - 2.81AB - 2.48AC - 1.15BC - 3.08A^2 - 0.31B^2 - 1.48C^2 \quad (3)$$

where *A* is the reaction temperature (°C), *B* is the reaction time (min), and *C* is the water-to-biomass ratio; *AB*, *AC*, and *BC* represent the interaction terms of the factors; and A^2, B^2, and C^2 represent the quadratic terms of the factors.

The theoretical values of the score obtained by calculating the mathematical model are close to the experimental values (Fig. 2). The coefficient of determination (R^2) is 0.9477, which indicates that the developed model shows a good effect in linking the correlation for the variables of HTC with the synthetic score. The statistical significance of the response surface quadratic model of the synthetic score from the hydrochar of MSs was estimated using ANOVA (Table 3). The model F value compares the model variance with

error variance; the P-value is the probability of seeing the observed F-value if the null hypothesis is true (Jung *et al*. 2016). The model produced an F-value of 14.09 and a P value of 0.0011, which indicates that the obtained mathematical model was significant. The P values of *A*, *B*, *AB*, *AC*, A^2, and C^2 were 0.0190, 0.0283, 0.0010, 0.0019, 0.0005, and 0.0215, respectively. These values suggest that the terms of *A*, *B*, *AB*, *AC*, A^2, and C^2 were significant ($P < 0.05$). According to the F-value, the linear term of reaction temperature (*A*) showed a more significant influence than those of reaction time and water-to-biomass ratio. Thus, the reaction temperature is a priority factor to consider when hydrothermal carbonation is performed.

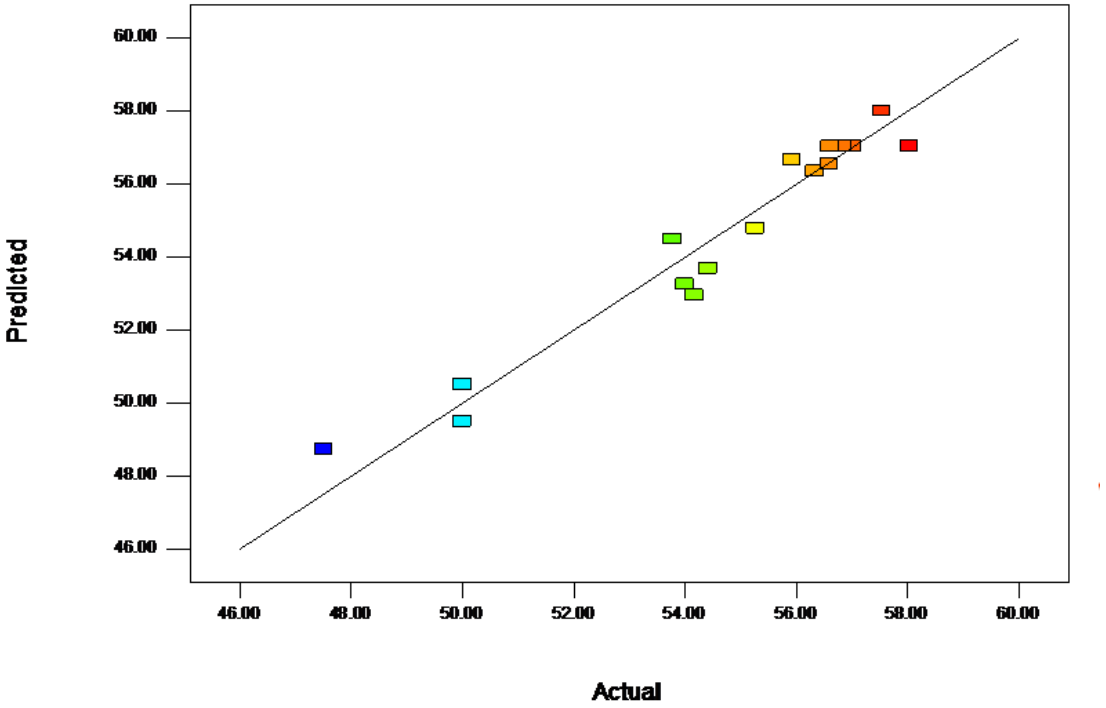

Fig. 2. Actual and predicted values of the synthetic score

Table 3. ANOVA for the Comprehensive Evaluation Score

Source	Sum of Squares	DF	Mean Square	F Value	P Value	Status
Model	134.91	9	14.99	14.09	0.0011	Significant
A	9.79	1	9.79	9.20	0.0190	
B	8.08	1	8.08	7.60	0.0283	
C	2.92	1	2.92	2.74	0.1418	
AB	31.64	1	31.64	29.74	0.0010	
AC	24.60	1	24.60	23.13	0.0019	
BC	5.31	1	5.31	4.99	0.0605	
A^2	39.83	1	39.83	37.44	0.0005	
B^2	0.41	1	0.41	0.39	0.5532	
C^2	9.23	1	9.23	8.68	0.0215	
Residual	7.45	7	1.06			
Lack of fit	6.12	3	2.04	6.13	0.0561	Not significant
Pure error	1.33	4	0.33			
Total	142.36	16				

The effect and relationship of parameters on the synthetic score can be expressed as 3D surfaces (Fig. 3). The 3D surface plot shows a classification of the surface shape for the various parameters. The synthetic score increased with increasing temperature and time (Fig. 3a). Nonetheless, when the temperature was above 220 °C, the synthetic score decreased after 120 min due to the remarkable effect of temperature during HTC.

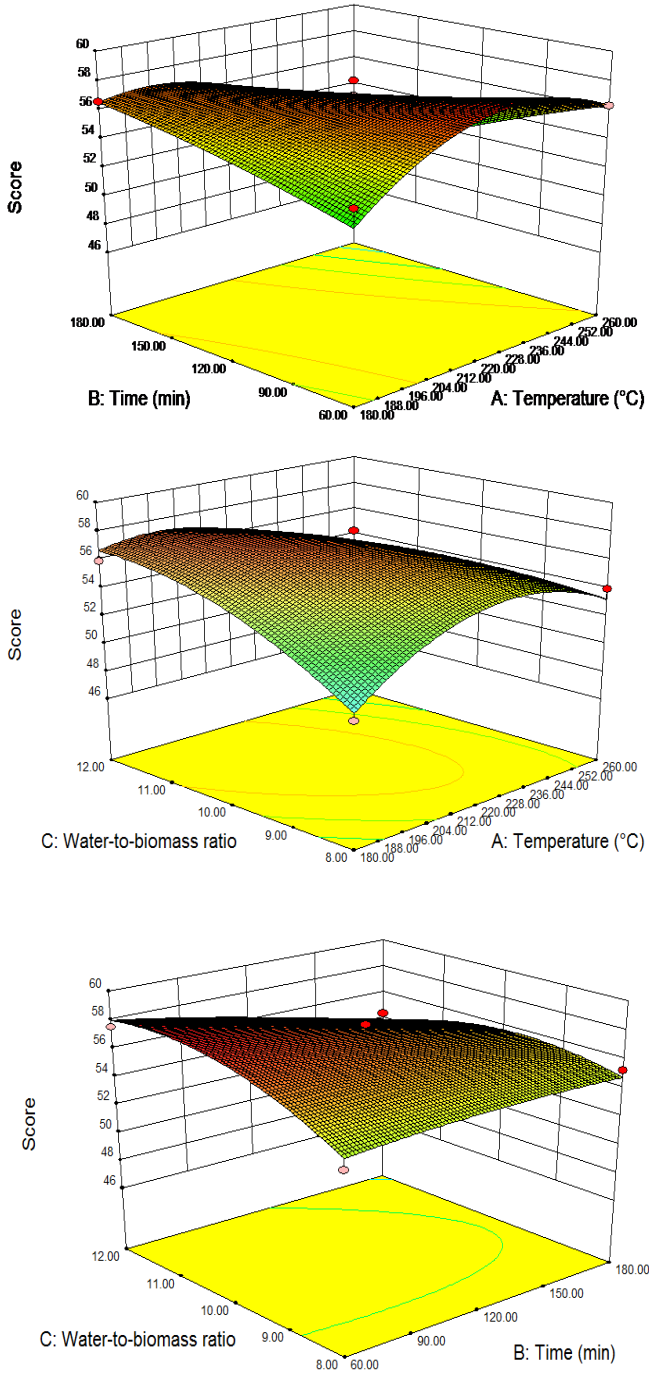

Fig. 3. Response surface on the synthetic score. Effect of (a) temperature and time, (b) temperature and water-to-biomass ratio, and (c) time and water-to-biomass ratio

The relationship between synthetic score and temperature and water-to-biomass ratio (Fig. 3b) showed a maximum on the response surface shape at a temperature of 220 °C and water-to-biomass ratio of 11. The relationship between synthetic score and time and water-to-biomass ratio (Fig. 3c) indicates that the interaction between time and water-to-biomass ratio is not evident.

Table 2 shows the highest hydrochar yield (run 5) and highest HHV (run 8) in the HTC of MSs. However, yield and HHV have an inverse relationship. Applying the synthetic weighted scoring method is necessary to solve the contradiction between the yield and HHV. The obtained mathematical model indicated that the optimal conditions for optimal response surface results are a temperature of 222.3 °C, time of 60 min, and water-to-biomass ratio of 11.1. The response score value is 58.3 at these conditions. The following conditions were defined to simplify the experimental conditions: temperature, 220 °C; time, 60 min; and water-to-biomass ratio of 11. The response score value is 58.1. Under these conditions, the hydrochar yield was 57.6%, and the HHV was 22.7 MJ/kg.

Chemical Properties and BET Analysis

The HHV, elemental, proximate, and BET analyses of the MSs and their hydrochar (hydrochar of optimum conditions) are listed in Table 4. The HHV values of the MSs and hydrochar were 18.78 and 25.9 MJ/kg, respectively. The HHV of hydrochar increased by 40% compared with MSs. This increase exceeds the HHV of lignite, and it is comparable with that of commercial coal (Liu *et al.* 2016; Wei *et al.* 2016). Compared with the hydrochar of *Camellia oleifera* shells (Fan *et al.* 2017b), HHV is lower, but the yield is higher.

Table 4. HHV, Elemental, Proximate, and Brunauer–Emmett–Teller (BET) Analyses of Raw Macadamia Shells (MSs) and Hydrochar at Optimum Conditions

Properties	MSs	Hydrochar at Optimum Condition
HHV(MJ/kg)	18.78	22.69
Elemental analysis		
Carbon (%)	52.60	56.41
Oxygen (%)[a]	40.53	37.49
Hydrogen (%)	6.02	5.32
Nitrogen (%)	0.74	0.68
Sulphur (%)	0.11	0.10
Proximate analysis		
Fixed carbon (%)	19.21	46.33
Volatile matter (%)	74.66	48.20
Moisture (%)	3.62	2.98
Ash (%)	2.51	2.49
BET analysis		
BET surface area (cm^2/g)	0.442	3.671
Total pore volume (cm^3/g)	0.001	0.018
Av. Pore diameter (nm)	0.957	2.476

[a] Oxygen content was obtained by using the difference.

Elemental analysis determines the composition and quantity of the gas removed during combustion and the amount of oxygen necessary to burn the biomass and fuels (Nizamuddin *et al.* 2016b). As illustrated in Table 4, the carbon content of the hydrochar increased by 7.24%, and the oxygen content decreased by 7.50% compared with raw MSs.

These results are mainly due to the decarboxylation and dehydration reactions during HTC; these reactions produce gases, mainly carbon dioxide, carbon monoxide, and hydrogen (Reza *et al.* 2015; Benavente *et al.* 2015).

This preliminary work aimed to optimise the parameters of HTC for suitable yield and HHV of hydrochar. Therefore, information from the proximate analysis of the MSs and hydrochar were compared. The proximate analysis results indicated that the volatile matter decreased from 74.7 % (MSs) to 48.2% (hydrochar). The fixed carbon content increased from 17.2% (MSs) to 46.3% (hydrochar). Results showed that the fuel characteristics of the hydrochar are dependent on the treatment conditions, and are improved as compared with those of raw MSs (He *et al.* 2013).

The surface area, total pore volume, and average pore diameter of the hydrochar increased compared with those of the raw MSs. This increase is attributed to the fibrous structure being destroyed during HTC, producing gas and liquid and leaving some microporous structures (Jain *et al.* 2015; Laginhas *et al.* 2016). Nevertheless, the microporous structure is very small compared with that of biochar from pyrolysis (Fan *et al.* 2017b).

SEM and FTIR Analyses

The physical structures of the hydrochar and the raw MSs are shown in Fig. 4. The MS structure was changed after HTC. Loose structures appeared on the surface of the hydrochar compared with the compact structure of MSs (Fig. 1b). Moreover, a few pores are present on the surface of the hydrochar. This effect was confirmed by the BET analysis results presented in Table 4, and it is explained by the degradation and polymerisation of cellulose and hemicelluloses (Fan *et al.* 2017b). However, microspheres were not observed on the hydrochar surface, which is mainly due to low reaction temperature and less reaction time, for which condensation, polymerisation, and aromatisation reactions do not occur.

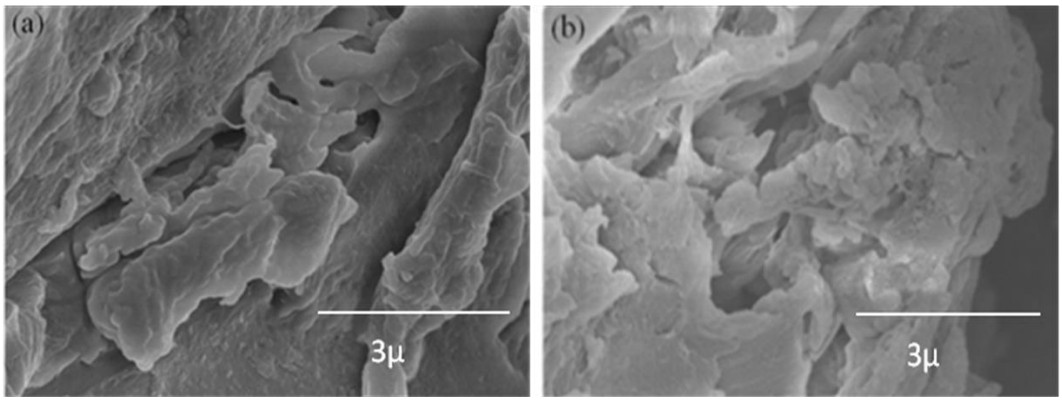

Fig. 4. Scanning electron microscopy images of raw MSs (a) and their hydrochar (b) at optimum conditions

The surface functional groups of the hydrochar and MSs were analysed by FTIR spectra at wave numbers ranging from 4000 cm^{-1} to 400 cm^{-1}, as shown in Fig. 5. The FTIR spectra of the hydrochar and MSs exhibited an evident change. The O–H (3450^{-1}) stretching vibration of the hydrochar was weaker than that of MSs because of the degree of deoxygenation and dehydration (Fan *et al.* 2017b). The bands of the hydrochar and MSs at 2895^{-1} ($–CH_2$ and$–CH_3$) showed no obvious difference. The results indicated that demethoxylation and demethylation of lignin occur infrequently at the optimum

conditions. The band at 1750 cm^{-1} is due to a stretching vibration of C=O in the FTIR spectra of MSs; this band disappeared after HTC, which suggests that the decarboxylation of hemicelluloses and cellulose is severe (Reza *et al.* 2014). The spectrum ranging from 1525 $cm^{-1}$to 500 cm^{-1} was mainly due to the stretching vibration of C=C, C–H, C–O–C, and C=O, which showed no significant difference.

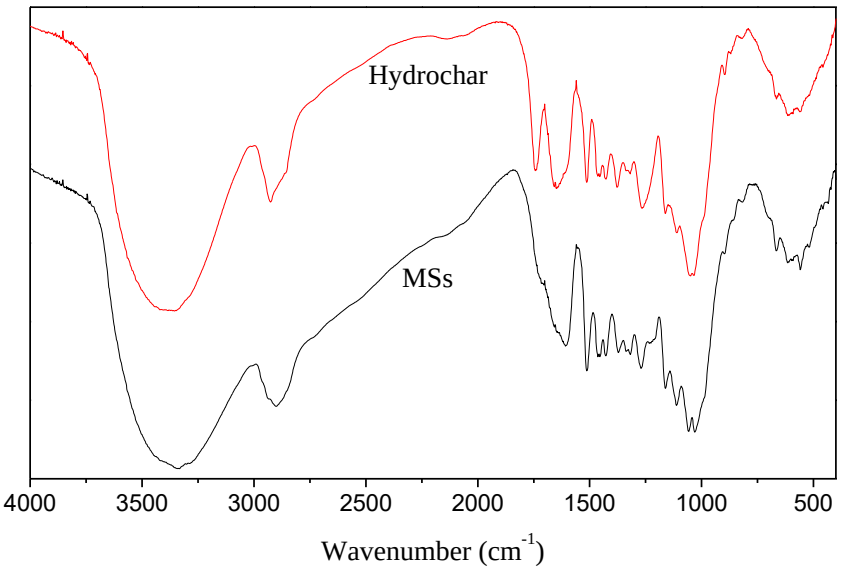

Fig. 5. Fourier transform infrared spectra of MSs and their hydrochar at optimum conditions

CONCLUSIONS

1. MSs can be used to produce hydrochar as fuel *via* HTC. The yield and HHV are influenced by reaction temperature, reaction time, and water-to-biomass ratio. The synthetic weighted scoring method was used as the response value because of opposition between the yield and HHV of hydrochar. An RSM analysis showed that reaction temperature is the most significant variable. According to the RSM model, the predicted maximum response value of 58.1 was obtained under optimum conditions (temperature, 220 °C; time, 60 min; and water-to-biomass ratio, 11).
2. Under optimal conditions, the hydrochar yield and HHV were 57.6% and 22.7 MJ/kg, respectively. The elemental and proximate analyses showed that the fuel properties of hydrochar from MSs were improved compared with raw MSs. BET, SEM, and FTIR analyses showed that the surface structure and functional groups of hydrochar also changed.

ACKNOWLEDGEMENTS

This work was supported by the National Natural Science Foundation of China (No. 31670599, No. 31160147), the 948 Project of State Forestry Administration of China (No. 2013-4-08), the Major Project of New Energy (No. 5 [2015]), Yunnan Province, China, and the Major Project (No. ZD2014012) of Education Department of Yunnan Province, China.

REFERENCES CITED

Abdulrazzaq, H., Jol, H., Husni, A., and Abubakr, R. (2014). "Characterization and stabilisation of biochars obtained from empty fruit bunch, wood, and rice husk," *BioResources* 9(2), 2888-2898. DOI: 10.15376/biores.9.2.2888-2898

Álvarez-Murillo, A., Román, S., Ledesma, B., and Sabio, E. (2015). "Study of variables in energy densification of olive stone by hydrothermal carbonization," *Journal of Analytical and Applied Pyrolysis* 113, 307-314. DOI: 10.1016/j.jaap.2015.01.031

Benavente, V., Calabuig, E., and Fullana, A. (2015). "Upgrading of moist agro-industrial wastes by hydrothermal carbonization," *Journal of Analytical and Applied Pyrolysis* 113, 89-98. DOI: 10.1016/j.jaap.2014.11.004

Fan, F., Zheng, Y., Huang, Y., Lu, Y., Wang, Z., Chen, B., and Zheng, Z. (2017a). Combustion kinetics of biochar prepared by pyrolysis of macadamia shells," *BioResources* 12(2), 3918-3932. DOI: 10.15376/biores.12.2.3918-3932

Fan, F., Zheng, Y., Huang, Y., Lu, Y., Wang, Z., Chen, B., and Zheng, Z. (2017b). "Preparation and characterization of biochars from waste *Camellia oleifera* shells by different thermo-chemical processes," *Energy & Fuels* 31 (8), 8146-8151. DOI: 10.1021/acs.energyfuels.7b00269

Ferdosian, F., Yuan, Z., Anderson, M., and Xu, C. (2014). "Synthesis of lignin-based epoxy resins: Optimization of reaction parameters using response surface methodology," *Rsc Advances* 4(60), 31745-31753. DOI: 10.1039/C4RA03978E

He, C., Giannis, A., and Wang, J. Y. (2013). "Conversion of sewage sludge to clean solid fuel using hydrothermal carbonization: Hydrochar fuel characteristics and combustion behavior," *Applied Energy* 111(11), 257-266. DOI: 10.1016/j.apenergy.2013.04.084

Jain, A., Balasubramanian, R., and Srinivasan, M. P. (2015). "Production of high surface area mesoporous activated carbons from waste biomass using hydrogen peroxide-mediated hydrothermal treatment for adsorption applications," *Chemical Engineering Journal* 273, 622-629. DOI: 10.1016/j.cej.2015.03.111

Jain, A., Balasubramanian, R., and Srinivasan, M. P. (2016). "Hydrothermal conversion of biomass waste to activated carbon with high porosity: A review," *Chemical Engineering Journal* 283, 789-805. DOI: 10.1016/j.cej.2015.08.014

Jung, K. A., Nam, C. W., Woo, S. H., and Park, J. M. (2016). "Response surface method for optimization of phenolic compounds production by lignin pyrolysis," *Journal of Analytical and Applied Pyrolysis* 120, 409-415. DOI: 10.1016/j.jaap.2016.06.011

Kambo, H. S., and Dutta, A. (2014). "Strength, storage, and combustion characteristics of densified lignocellulosic biomass produced *via* torrefaction and hydrothermal carbonization," *Applied Energy* 135, 182-191. DOI: 10.1016/j.apenergy.2014.08.094

Kambo, H. S., and Dutta, A. (2015). "Comparative evaluation of torrefaction and hydrothermal carbonization of lignocellulosic biomass for the production of solid biofuel," *Energy Conversion & Management* 105, 746-755. DOI:10.1016/j.enconman.2015.08.031

Kim, D., Lee, K., and Park, K. Y. (2016). "Upgrading the characteristics of biochar from cellulose, lignin, and xylan for solid biofuel production from biomass by hydrothermal carbonization," *Journal of Industrial & Engineering Chemistry* 42, 95-100. DOI: 10.1016/j.jiec.2016.07.037

Kumar, U., Maroufi, S., Rajarao, R., Mayyas, M., Mansuri, I., Joshi, R., and Sahajwalla, V. (2017). "Cleaner production of iron by using waste macadamia biomass as a carbon resource," *Journal of Cleaner Production* 158, 218-224. DOI:

10.1016/j.jclepro.2017.04.115

Laginhas, C., Nabais, J., and Titirici M. M. (2016). "Activated carbons with high nitrogen content by a combination of hydrothermal carbonization with activation," *Microporous & Mesoporous Materials* 226, 125-132. DOI: 10.1016/j.micromeso.2015.12.047

Lei, Z., Qiang, W., Wang, B., Yang, G., Lucia, L. A., and Chen, J. (2015). "Hydrothermal carbonization of corncob residues for hydrochar production," *Energy & Fuels* 29(2), 872-867. DOI: 10.1021/ef502462p

Liu, H. M., Xie, X. A., Li, M. F., and Sun, R. S. (2012). "Hydrothermal liquefaction of cypress: effects of reaction conditions on 5-lump distribution and composition," *Journal of Analytical and Applied Pyrolysis* 94(6), 177-183. DOI: 10.1016/j.jaap.2011.12.007

Liu, F. J., Wei, X. Y., Fan, M., and Zong, Z. M. (2016). "Separation and structural characterization of the value-added chemicals from mild degradation of lignites: A review," *Applied Energy* 170, 415-436. DOI: 10.1016/j.apenergy.2016.02.131

Mau, V., Quance, J., Posmanik, R., and Gross, A. (2016). "Phases' characteristics of poultry litter hydrothermal carbonization under a range of process parameters," *Bioresource Technology* 219, 632-642. DOI: 10.1016/j.biortech.2016.08.027

Nizamuddin, S., Mubarak, N. M., Tiripathi, M., Jayakumar, N. S., Sahu, J. N., and Ganesan, P. (2015). "Chemical, dielectric and structural characterization of optimized hydrochar produced from hydrothermal carbonization of palm shell," *Fuel*, 163.88-97.DOI:org/10.1016/j.fuel.2015.08.057

Nizamuddin, S., Shrestha, S., Athar, S., Ali, B. S., and Siddiqui, M. A., (2016a). "A critical analysis on palm kernel shell from oil palm industry as a feedstock for solid char production," *Reviews in Chemical Engineering* 32(5), 489-505. DOI: 10.1515/revce-2015-0062

Nizamuddin, S., Mubarak, N. M., Tiripathi, M., Jayakumar, N. S., Sahu, J. N., and Ganesan, P. (2016b). "Chemical, dielectric and structural characterization of optimized hydrochar produced from hydrothermal carbonization of palm shell," *Fuel* 163, 88-97. DOI: 10.1016/j.fuel.2015.08.057

Nizamuddin, S., Baloch, H. A., Griffin, G. J., Mubarak, N. M., Bhutto, W. A., Abro, R., Mazari, S., and Ali, B. (2017). "An overview of effect of process parameters on hydrothermal carbonization of biomass," *Renewable & Sustainable Energy Reviews* 73, 1289-1299. DOI: 10.1016/j.rser.2016.12.122

Peng, C., Zhai, Y., Zhu, Y., Xu, B., Wang, T., Li, C., and Zeng, G. (2016). "Production of char from sewage sludge employing hydrothermal carbonization: Char properties, combustion behavior and thermal characteristics," *Fuel* 176, 110-118. DOI: 10.1016/j.fuel.2016.02.068

Rajarao, R., and Sahajwalla, V. (2016). "A cleaner sustainable approach for synthesising high purity silicon carbide and silicon nitride nanopowders using macadamia shell waste," *Journal of Cleaner Production* 133, 1277-1282. DOI: 10.1016/j.jclepro.2016.06.029

Reza, M. T., Wirth, B., Lüder, U., and Werner, M. (2014). "Behavior of selected hydrolyzed and dehydrated products during hydrothermal carbonization of biomass," *Bioresource Technology* 169(5), 352-361. DOI: 10.1016/j.biortech.2014.07.010

Reza, M. T., Rottler, E., Herklotz, L., and Wirth, B. (2015). "Hydrothermal carbonization (HTC) of wheat straw: Influence of feedwater pH prepared by acetic acid and potassium hydroxide," *Bioresource Technology* 182, 336-344. DOI: 10.1016/j.biortech.2014.07.010

Thangalazhy-Gopakumar, S., Al-Nadheri, W. M. A., Jegarajan, D., Sahu, J. N., Mubarak, N. M., and Nizamuddin, S. (2015). "Utilization of palm oil sludge through pyrolysis for bio-oil and bio-char production," *Bioresource Technology* 178, 65-69. DOI:10.1016/j.biortech.2014.09.068

Wechsler, A., Zaharia, M., Crosky, A., Jones, H., Ramirez, M., Ballerini, A., Nuñez, M., and Sahajwalla, V. (2013). "Macadamia (*Macadamia integrifolia*) shell and castor (*Rícinos communis*) oil based sustainable particleboard: A comparison of its properties with conventional wood based particleboard," *Materials & Design* 50, 117-123. DOI: 10.1016/j.matdes.2013.03.008

Wei, Y., Hui, W., Meng, Z., Zhu, J. Y., and Zhou, J. (2016). "Fuel properties and combustion kinetics of hydrochar prepared by hydrothermal carbonization of bamboo," *Bioresource Technology* 205, 199-204. DOI: 10.1016/j.biortech.2016.01.068

Wongcharee, S., Aravinthan, V., Erdei, L., and Sanongraj, W. (2017). "Use of macadamia nut shell residues as magnetic nanosorbents," *International Biodeterioration & Biodegradation* 124, 276-287. DOI: 10.1016/j.ibiod.2017.04.004

Xing, X., Fan, F., Shi, S., Xing, Y., Li, Y., and Zhang, X. (2016). "Fuel properties and combustion kinetics of hydrochar prepared by hydrothermal carbonization of corn straw," *BioResources* 11(4), 9190-9204. DOI: 10.15376/biores.11.4.9190-9204

Yang, W., Shimanouchi, T., Iwamura, M., Takahashi, Y., Mano, R., Takashima, K., tanifuji, T., and Kimura, Y. (2015). "Elevating the fuel properties of *Humulus lupulus*, *Plumeria alba*, and *Calophyllum inophyllum*, L. through wet torrefaction," *Fuel* 146, 88-94. DOI: 10.1016/j.fuel.2015.01.005

Zhao, X., Xiong, L., Zhang, M., and Bai, F. (2016). "Towards efficient bioethanol production from agricultural and forestry residues: Exploration of unique natural microorganisms in combination with advanced strain engineering," *Bioresource Technology* 215, 84-91. DOI: 10.1016/j.biortech.2016.03.158

Zheng, Y., Wang, Y., Lu, Y., Hu, Y. S., and Li, J. (2017). "A high-performance sodium-ion battery enhanced by macadamia shell derived hard carbon anode," *Nano Energy* 39, 489-498. DOI: 10.1016/j.nanoen.2017.07.018

Article submitted: September 28, 2017; Peer review completed: November 25, 2017; Revised version received and accepted: December 2, 2017; Published: December 7, 2017.
DOI: 10.15376/biores.13.1.967-980